HHS Public Access

Author manuscript

J Gastrointest Surg. Author manuscript; available in PMC 2018 January 01.

Published in final edited form as:

J Gastrointest Surg. 2017 January ; 21(1): 94–105. doi:10.1007/s11605-016-3222-z.

Restitution of Tumor Suppressor microRNA-145 using Magnetic Nanoformulation for Pancreatic Cancer Therapy

Saini Setua[1], **Sheema Khan**[1], **Murali M. Yallapu**[1], **Stephen W. Behrman**[2], **Mohammed Sikander**[1], **Shabia Shabir Khan**[3], **Meena Jaggi**[1], and **Subhash C. Chauhan**[1]

[1]Department of Pharmaceutical Sciences and Center for Cancer Research, University of Tennessee Health Science Center, Memphis, Tennessee, USA

[2]Department of Surgery, University of Tennessee Health Science Center, Memphis, Tennessee, USA

[3]Department of Computer Science, University of Kashmir, Srinagar, Jammu and Kashmir, India

Abstract

Introduction—The functional significance of lost microRNAs has been reported in several human malignancies, including pancreatic cancer (PC). Our prior work has identified microRNA-145 (miR-145) as a tumor suppressor microRNA (miRNA) in pancreatic cancer. The restoration of miR-145 downregulates a number of oncogenes including mucin MUC13, a transmembrane glycoprotein that is aberrantly expressed in pancreatic cancer, thus efficiently inhibiting tumor growth in mice. However, lack of an effective tumor specific delivery system remains an unmet clinical challenge for successful translation of microRNAs.

Methods—We developed a miRNA-145 based magnetic nanoparticle formulation (miR-145-MNPF) and assessed its anti-cancer efficacy. Physico-chemical characterization, (DLS; Dynamic light scattering, TEM; Transmission electron microscopy, miR binding efficiency), cellular internalization (Prussian blue, confocal microscopy), miR-145 restitution potential (qRT-PCR) and anti-cancer efficacy (proliferation, colony formation, cell migration, cell invasion assays) of this formulation were performed using clinically relevant pancreatic cancer cell lines (HPAF-II, AsPC-1).

*Corresponding Authors: Subhash C. Chauhan, Ph.D., Professor, Department of Pharmaceutical Sciences, University of Tennessee Health Science Center, 19 South Manassas, Cancer Research Building, Memphis, TN, 38163. Phone: (901) 448-2175. Fax: (901) 448-1051. schauha1@uthsc.edu.

Author Contribution

All the authors listed in the manuscript (Saini Setua, Sheema Khan, Murali M. Yallapu, Stephen W. Behrman, Mohammed Sikander, Shabia Shabir Khan, Meena Jaggi, Subhash C. Chauhan) contributed to following.

- Substantial contributions to the conception or design of the work; or the
- Acquisition, analysis, or interpretation of data for the work; AND
- Drafting the work or revising it critically for important intellectual content; AND
- Final approval of the version to be published; AND
- Agreement to be accountable for all aspects of the work in ensuring that questions related to the accuracy or integrity of any part of the work are appropriately investigated and resolved.

Potential conflicts of interest

The authors declare that there are no financial and non-financial competing interests.

Results—miR-145-MNP formulation exhibited optimal particle size and zeta potential which effectively internalized and restituted miR-145 in pancreatic cancer cells. miR-145 re-expression resulted in downregulation of MUC13, HER2, pAKT and inhibition of cell proliferation, clonogenicity, migration, and invasion of pancreatic cancer cells.

Conclusions—miR-145-MNP formulation is an efficient system for miR-145 delivery and restitution in pancreas cancer that may offer a potential therapeutic treatment for PC either alone, or in conjunction with conventional treatment.

Keywords

Magnetic nanoparticle; miR-145; pancreatic cancer; therapeutics; nanotherapies

Introduction

Pancreatic cancer remains a highly lethal human malignancy due to a failure of effective adjuvant therapies [1]. MicroRNAs (miRNA) are small noncoding RNAs that regulate multiple biological pathways during cancer development and progression and serve as tumor suppressors or oncogenes. The inhibition of oncogenic microRNAs using anti-miRs and restitution of tumor suppressor microRNAs *via* miRNA mimics represent a powerful therapeutic strategy in cancer treatment [2, 3]. Prior work from our lab and that of others have demonstrated the tumor suppressor role of miR-145 in pancreatic cancer [4,5–7]. Our study has shown that miR-145 targets a newly identified transmembrane glycoprotein, MUC13 that is aberrantly expressed in pancreatic cancer and modulates its associated targets, such as HER2, pAKT^{Ser473} and p53 [4]. Its restoration inhibits MUC13 levels and suppressed tumor growth in pancreatic cancer xenograft mice model [4]. Although studies provide compelling evidence for miR-145 involvement in the inhibition of pancreatic cancer, the impact of its sustained release has not been established. Obstacles to the successful and efficient delivery of microRNAs for therapy have yet to be overcome.

Magnetic nanoparticle formulations for drug delivery have previously been generated but due to the high particle size in suspension, loss of magnetization and inefficient internalization in the target cells resulted in poor therapeutic efficacy for cancer treatment [8]. Recently, we have engineered a unique magnetic nanoparticle (MNP) based system for gene(s) and drug(s) delivery applications [8–10]. We have previously demonstrated that our uniquely engineered MNPs are capable of targeting pancreatic tumors efficiently with the help of the “Enhanced Permeation and Retention” (EPR) effect [9] leading to increased cellular uptake and internalization of MNPs in cancer cells. EPR effect is a unique phenomenon of tumors based on their pathophysiological differences from normal tissues, particles of certain sizes are capable of accruing and retaining selectively in tumor tissues but not in normal tissue. Additionally, these MNPs have shown enhanced MRI properties (compared to conventional MNPs) [10]. Polyethylenimines (PEIs) are linear or branched polymers being partially protonated under physiological conditions, that easily form complexes with nucleic acids [11]. PEIs have previously been shown to be excellent delivery vehicles for DNA plasmids and other DNA or RNA molecules including ribozymes and siRNAs [11]. The purpose of this study was to generate a miRNA-145 loaded magnetic nanoparticle system utilizing our recently engineered MNPs and assess the efficacy of this

formulation for miR-145 restitution and its role in the potential treatment of pancreatic cancer.

Materials and Methods

Culture of pancreatic cancer cells

Human pancreatic cancer cells, HPAF-II and AsPC-1 were purchased from American Type Cell Culture (ATCC; Manassas, VA, USA) and cultured using cell specific culture media, F12/DMEM and RPMI (HyClone Laboratories, Inc. South Logan, Utah, USA), respectively, which was supplemented with 10% fetal bovine serum (Atlanta Biologicals, GA, USA) and antibiotic/antimycotic solution at 37 °C in a humidified atmosphere (5% CO2 and 95% air atmosphere). Cells were routinely tested for mycoplasma every six months.

Chemicals, reagents, microRNA mimics and antibodies

All chemicals and reagents were purchased from Sigma Adrich Corporation (St. Louis, MO, USA) and cell culture wares were purchased from Corning life sciences (Tewksbury MA, USA). Non-targeting control (catalog number: AM17111) and miR-145 mimics (catalog number: 4464066), Taqman miR-145 probes (Assay id: 002278), High Capacity cDNA Reverse Transcription kit (catalog number: 4368814) and TRIzol reagent (catalog number: AM 9738) were purchased from Life technologies (Carlsbad, CA, USA). The primary antibodies, anti-HER2 (catalog number: 2165S), $pAKT^{Ser473}$ (catalog number: 9271) and anti-p53 (catalog number: 2527) were purchased from Cell Signaling (Danvers, MA, USA) and anti-β–actin (catalog number: A5316) was purchased from Sigma (St. Louis, MO, USA).

Preparation of miR-145-MNPF formulation

Iron oxide nanoparticles were prepared by the co-precipitation using Fe^{2+} (300 mg) and Fe^{3+} (800 mg) ions in the molar ratio ~ 1:2 as described previously [9]. Briefly, 200 mg of β-cyclodextrin (β-CD) was added to the solution and stirred for 10 mins at 500 rpm. 250 mg of Pluronic F-127 was added to the suspension and stirred overnight followed by washing the particles thrice and re-suspending in water. In this study, we used PEI for the purpose of miR-145 delivery as these polycationic polymers form non-covalent complexes with nucleic acids and aid in efficient gene delivery [12]. In order to form a uniform layer, 100 mg PEI was added to the MNP suspension and stirred overnight. These MNP-PEI nanoparticles are stored and loaded with microRNA mimics just prior to treatment of the cells. 100 nM of non-targeting experimental control (NC) or miR-145 mimics were incubated with 1μg/ml of MNP-PEI nanoparticles in 0.9% Nacl for 30 min to form NC-MNPF (non-targeting control-MNP formulation) and miR-145-MNPF (miR-145-MNP formulation) complex [8].

Particle size and zeta potential

The hydrodynamic nanoparticle size and zeta (ζ) potential of miR-145-MNPF were determined by the dynamic light scattering (DLS) principle using Zetasizer (Nano ZS, Malvern Instruments, Malvern, UK). To measure the particle size 25 μL of 1 mg/ml nanoparticle suspension was added to 3 ml of water and probe sonicated using VirSonic

Ultrasonic Cell Disrupter 100 128 (VirTis, Gardiner, NY) for 30 seconds. For ζ-potential measurement, the same diluted particle suspension were used.

Transmission electron microscopy

The size and morphology of magnetic miR-145-MNPF were determined by JEOL 200EX transmission electron microscopy (TEM) (JEOL Ltd, Tokyo, Japan) operating at 60 kV. 100 μg/ml nanoparticle suspension was prepared and probe sonicated for 30 sec. 200 mesh formvar-coated copper TEM grid (grid size: 97 μm; Ted Pella Inc, Redding, CA, USA) was used to prepare samples by carefully placing the nanoparticle suspension (20 μl) on the dark side of grid. The excess amount of formulation was removed by filter paper and the grid was allowed to air dry followed by imaging.

Gel retardation assay

The complex formation of MNPs with miR-145 was determined by the gel retardation assay using MNPs and miR-145 at different ratios. 1–10 μg of MNPF was incubated for 30 minutes with 100 nM of miR-145 mimic. Gel electrophoresis was performed using 2% agarose gel that was allowed to run for 1 hour at different time intervals and photographed the gel to check the particle movement as described earlier [13].

Cellular treatment with MNPF

HPAF-II and AsPC-1 cells were seeded in 24 well plates at 60 – 70% confluency. Cells were treated with experimental controls (MNPs, NC-MNPF) or miR-145-MNPF and incubated up to 48 hours. After 48 hours of transfection, cells were used to investigate the functional effects of transfection on proliferation, migration and invasion.

Cellular uptake

Prussian blue staining was used to determine the cellular uptake of MNP formulations in the pancreatic cancer cells. Cells were seeded in 24 well plate followed by transfection with NC-MNPF and miR-145-MNPF. After 24 hours, Prussian blue staining reagent was added to the cells. After 30 min the cells were washed with PBS and the images were captured using phase contrast microscopy to determine the uptake of iron particle inside the cells [10].

Proliferation assay

Cell proliferation assay was performed to investigate the effect of miR-145-MNPF by using the Cell Counting Kit-8 (Mayflower Bioscience) and a microplate reader (Cytation 3, BioTek, Winooski, VT, USA), as described earlier [14]. Briefly, pancreatic cancer cells (5×10^3/ well) were seeded in 96 well plate and allowed overnight followed by treatment with MNPF, NC-MNPF, miR-145-MNPF and incubation for 48 hrs at 37 °C. The anti-proliferative effect of each treatment was calculated as a percentage of cell growth with respect to the control (NC-MNPF) [8].

Additionally, cell viability assay was performed in HPAF-II and AsPC-1 cells after treatment with NC-MNPF and miR-145-MNPF. Following 48 hours of treatment, cells were trypsinized and counted in triplicates, using cell countess equipment (Invitrogen). Data were plotted as a percentage of cell growth with respect to the control (NC-MNPF).

qPCR of miR-145

Following transfection of cells with NC-MNPF and miR-145-MNPF, total RNA was extracted using TRIzol reagent. RNA was quantified using Nanodrop instrument 2000 (Thermo Scientific). 50 ng of RNA reverse transcribed into cDNA using specific RT primers for miR-145 and High Capacity cDNA Reverse Transcription kit. The changes in the expression level of miR-145 was determined by real-time polymerase chain reaction using Taqman PCR master mixture and Taqman probes. RNUB6 was used as an endogenous control for the experiment [4].

Clonogenicity assays

Colony formation assay was performed to investigate the effect of miR-145-MNPF on the colony forming ability of pancreatic cancer cells, as described previously [15]. Briefly, HPAF-II and AsPC-1 cells were transfected with MNPF, NC-MNPF and miR-145-MNPF. After transfection, cells were trypsinized and re-plated (250×10^2/ well) in 12 well plate for 2 weeks. Colonies were fixed, stained with crystal violet and photographed. Colonies were counted manually and plotted as a percent clonogenicity. Control colonies were considered as 100%.

Cell migration and motility assays

Cell migration was analyzed using scratch assay, as described before [14]. Briefly, following transfection with MNPF, NC-MNPF and miR-145-MNPF, HPAF-II and AsPC-1 cells were plated to form a monolayer. Cell monolayer was scraped using a micropipette tip and allowed to incubate and the residual gap length calculated from photomicrographs at the initial time (0hr) and after 24hrs.

Cellular motility was determined by agarose bead-based cell motility assay. MNP, NC-MNPF and miR-145-MNPF transfected cells were trypsinized and mixed with 0.4% low melting agarose solution. 20μL of cells-agarose solution was placed onto the fibronectin/ BSA coated plate, each agarose bead containing about 20000 to 30000 cells. Then the plate was placed at 4°C for 7 min to solidify the agarose beads. Complete cell culture media was added to the wells carefully followed by incubation for 3 to 4 days. The plates were photographed for migrated cells using phase contrast microscope at day 0 and 3 [16].

Cell invasion assay

Cell Invasion assay was performed to investigate the effect of miR-145-MNPF on the cells using BD Biocoat Matrigel Invasion Chambers (BD Biosciences) [14], as per manufacturer's protocol. After 48 hours incubation, the invading cells were fixed with methanol and stained with crystal voilet. The invaded cells were counted and plotted as percent invasion of the miR-145 treated cells compared to control (MNPF and NC-MNPF).

Real time cell proliferation, migration and invasion assays through xCELLigence system

To further confirm effects of MNPF on cellular growth and motility and invasiveness, real-time migration, invasion and proliferation assays were performed using the xCELLigence system as described earlier [14]. xCELLigence system is an electrical impedance-based

method that allows for the measurement of cell migration, invasion and proliferation in real-time. Briefly cells (HPAF-II, AsPC-1) were seeded per chamber of cell proliferation (4×10^3) or invasion and migration (4×10^4) plate and the cells after treatment with miR-145 MNPF or empty MNPF were analyzed in xCELLigence instrument at 37°C, 5% CO_2 for real time cell proliferation, migration and invasion assays.

Western blotting

HPAF-II and AsPC-1 cells were transfected with NC-MNPF and miR-145- MNPF. Whole cell lysate were prepared and Western blotting was performed as described earlier [17]. Expression of protein was analyzed by immunoblotting with specific antibodies, anti-MUC13 MAb, anti-HER2, $pAKT^{Ser473,}$ anti-p53 and anti-β–actin.

Hemocompatibility assay

To determine the hemocompatibility of miR-145-MNPF, the blood collected from a healthy donor was used (Biological Specialty Corp; Colmar, PA). The whole blood was centrifuged at 2000 rpm for 10min, supernatant discarded and Red blood cells (RBCs) were collected for hemolysis assay. The RBCs were re-suspended in 10 ml of PBS and 100 μl of cell suspension was treated with different concentrations of MNPF followed by incubation for 2 hrs at 37 °C. PBS and sodium dodecyl sulfate (SDS) were used as negative and positive experimental controls, respectively. After incubation, the treated cells were centrifuged and degree of hemolysis was analyzed in the collected supernatant using spectrophotometer (Cytation 3, BioTek) at λ_{max} 570 nm [8].

Statistical analysis

The data were processed using Microsoft Excel and presented as mean±standard error of the mean (SEM). Statistical significance of the data was performed by a Student's t test. The level of significance was set at $*p < 0.05$.

Results

Generation of miR-145-MNP nanoformulation

The miR-145-MNPF was formulated as depicted in figure 1a and described earlier[8, 9]. PEI was used as a cationic polymer to increase the surface attachment of miR-145. Particle size and charge were identified by dynamic light scattering method. Optimal particle size (163 nm in DLS and 8–10 nm in TEM) and surface charge (30 mV) were determined for miR-145-MNPF (Fig. 1b–d). Additionally, we observed the complex formation of miR-145 with MNPs as seen in lane 5 and the complexation was further increased in lanes 6–9 with increase in the concentration of MNP (2–10 μg) (Fig. 1e). This indicated a complete retardation of mobility of the complexes formed, as visualized by reduced band intensity on complexation of miR-145 with MNPF (Fig. 1e).

miR-145-MNPF is less toxic and hemocompatible

To establish the potential clinical utility of any nanoformulation, evaluation of its general toxicity and hemocompatibility is utmost important. Therefore, we sought to determine the

toxicity of our delivery system (MNPF) and compared it with lipofectamine (Life technologies), the commonly used transfection reagent for nucleic acid delivery in a cell culture system. Treatment of human red blood cells with different concentrations of MNPF or lipofectamine indicated less or no toxicity of MNPF in RBCs, even at higher concentrations while lipofectamine was quite toxic as determined by spectroscopic analysis at λ_{max} 570 nm (Fig. 2a and b). Additionally, pancreatic cancer cells were treated with different concentrations of MNPF or lipofectamine for 48 hours to determine toxicity profile. Spectrophotometric analysis indicated that empty MNPF was not toxic to cancer cells whereas, lipofectamine showed significant toxicity (Fig. 2c). This data suggests that the MNPF is hemocompatible and PEI conjugation to MNP does not make the formulation toxic confirming that our MNPF is a safe delivery system for pre-clinical and clinical applications.

miR-145-MNPF effectively internalizes and restores miR-145 in pancreatic cancer cells

Effective internalization of particle into the cell or intracellular uptake of particle is a key factor to determine the therapeutic efficacy of a nanoparticle formulation. We investigated the cellular uptake/internalization and delivery efficacy of our miR-145-MNPF into the pancreatic cancer cells. Prussian blue staining of HPAF-II cells that were treated with NC-MNPF and miR-145-MNPF, demonstrate the efficient cellular uptake of the MNP formulations (Fig. 3a). Cellular internalization was also confirmed through Coumarin-6 dye loaded MNPs through confocal microscopy analysis (Fig. 3b). Coumarin-6-loaded MNPs efficiently internalized as indicated by high cytosolic staining and strong co-localization to the mitochondrial marker, mitotracker. Less co-localization of MNPs with early endosome and late endosome/lysosome markers indicated their escape from lysosomal degradation. Therefore, increased accumulation of MNPs was observed in mitochondria. This indicates that MNPs are able to escape from late endosome and lysosome compartments and reach into the cytosol/mitochondria for efficient functioning rather than undergoing a lysosome recycling process.

These findings are consistent with our previously published studies with drug loaded MNPs [9, 10]. The internalization of NC-miR-145 or miR-145-MNPF was almost equal to the MNP and that the miR-145 loading to MNPs did not affect the cellular uptake of these particles into the pancreatic cancer cells.

The expression level of miR-145 was assessed in HPAF-II and AsPC-1 cells that were treated with miR-145-MNPF by quantitative reverse-transcription PCR (qRT-PCR) assay (Fig. 3c). miR-145 expression was increased about 19 and 4 folds in AsPC-1 and HPAF-II cells, respectively, as compared to control groups (NC-MNPF). These results suggest that miR-145-MNPF can effectively deliver and restitute miR-145 into pancreatic cancer cells.

miR-145-MNPF inhibits tumorigenic features of pancreatic cancer cells

To investigate the effect of miR-145-MNPF on cell growth we performed cell proliferation and viability assays. Results demonstrated that miR-145-MNPF inhibited cell proliferation both in HPAF-II and AsPC-1 cells as compared to NC-MNPF treated cells (Fig. 4a). We further determined the effect of miR-145-MNPF on cell viability by counting the cells using Cell countess (Invitrogen) (Fig. 4b). It was observed that miR-145-MNPF treated cells

showed significantly decreased cellular viability (HPAF-II: 72 % and AsPC-1: 26 %) compared to the control (NC-MNPF) treated cells (Fig. 4b). We also studied the phenotypic changes occurring in pancreatic cancer cells on restoration of miR-145. The cells treated with miR-145-MNPF showed apparent change in morphology compared to control and NC-MNPF (Fig. 4c). Cells treated with miR-145-MNPF appeared relatively more circular in shape, loosely attached and grew in smaller patches. The effect of MNPF on cell proliferation was also confirmed in real time using xCELLigence system (Fig. 4d) which showed a similar growth inhibitory pattern. However, we observed slightly lower effect in AsPC-1 cells compared to HPAF-II cells at the same time point. Additionally, the results demonstrate that miR-145-MNPF markedly decreases clonogenicity in HPAF-II and AsPC-1 cells (by 77% and 59% respectively), compared to NC-MNPF treated cells (Fig. 4e). Altogether, these results clearly suggest that the miR-145-MNPF successfully delivers miR-145 into the cells which leads to the inhibition of cell proliferation, morphology and colony forming ability in pancreatic cancer cells.

miR-145-MNPF mediated delivery of miR-145 inhibits metastatic phenotypes of pancreatic cancer cells

To determine effects of miR-145-MNPF on metastatic characteristics of pancreatic cancer cells, cell migration and invasion assays were performed using HPFA-II and AsPC-1 cells. Matrigel invasion assay indicated inhibitory effects of miR-145-MNPF on the invasiveness of HPAF-II (80 %) and AsPC-1 (76 %) cells (Fig. 5a and b). Additionally, we investigated the effect of miR-145-MNPF on the cellular motility and migration in pancreatic cancer cells using wound healing and agarose bead assays (Fig. 6a and b). miR-145-MNPF demonstrated a significant inhibition of the cell migratory potential of HPAF-II and AsPC-1 cells both in agarose bead and wound healing assays as compared to control (NC-MNPF) treated cells. The effect of MNPF on cell migration and cell invasion was also confirmed in real time using xCELLigence system (Fig. 6c). This assay also showed a similar inhibitory effects on cell migration and cell invasion capability of aforementioned cells (Fig. 6c).

miR-145-MNPF targets MUC13 and regulates its downstream oncogenic signaling cascade

Considering potent anti-tumorigenic and anti-metastatic potential of miR-145-MNPF in functional assays, we sought to investigate its putative inhibitory molecular mechanisms. Thus, we evaluated the effect of miR-145-MNPF on the expression of MUC13, HER2, $pAKT^{Ser473}$ and p53 (Fig. 7a, b). Immunoblotting analysis data suggested that miR-145-MNPF effectively suppressed the expression of MUC13, $pAKT^{Ser473}$ and HER2 in HPAF-II and AsPC-1 cells. Contrary to this, however, miR-145-MNPF rescued the p53 expression levels. These data further validate the ability of miR-145-MNPF to effectively deliver miR-145 in pancreatic cancer cells accompanying the functional consequences via repression of its direct target MUC13 (Fig. 7c).

Discussion

This study describes engineering of a recently identified tumor suppressor miR-145[4] loaded unique magnetic nanoparticle formulation (miR-145-MNPF) for efficient delivery of a tumor suppressor miR-145. Our data demonstrated efficient cellular delivery, uptake/internalization

capability, restitution of miR-145 and potent anti-cancer effects of this novel miR-145-MNPF in pancreatic cancer cell line models. Successful delivery of microRNAs is governed by several processes that include high cellular uptake of the RNA, escape from lysosomal degradation, non-immunogenicity and stability in the bloodstream. The active routing of the delivered miRNA to the target organ and its entry into the cell is a determining factor for it to reach its intracellular target in an active form. For this purpose, generation of newer and improved delivery systems is highly desirable.

The therapeutic application of miR-145 has been previously evaluated in a xenograft model of pancreatic cancer [4]. A strong reduction in tumor growth was observed in mice receiving intra-tumoral miR-145 injection compared to the control treated group, which suggested its therapeutic potential for pancreatic cancer treatment[4]. We have generated a unique MNP based delivery vehicle for microRNAs that has been used in our previous studies to deliver anti-cancer drugs [9, 10, 8]. For the purpose of microRNA delivery, we have further engineered our magnetic nanoparticles by conjugating them with positively charged, branched PEI (MNPF). This enabled the surface attachment of miR-145 to the negatively charged MNPs with reduced toxicity effects of PEI. The use of branched PEI exhibits high transfection efficiency due to the high cationic charge for efficient gene delivery. The MNPF was found to be nontoxic and hemocompatible as it did not show any toxicity in RBCs. The probable reason of the reduced cytotoxicity of the PEI may be due to the presence of a layer of bio-adhesive material, Pluronic F127 that formulates it to render reduced toxic effects. It has previously been observed that Pluronic F127-PEI exhibits better condensation and complexation properties than PEI [18]. This strategy seems to provide a promising intervention of a stable, high transfection efficiency nanocarrier for microRNA delivery. Additionally, the use of a Pluronic F127 greatly improved the cellular uptake and reduced aggregation of the particles whereas the layer of β-cyclodextrin serves as a platform for simultaneous drug loading [9] which provides a feasibility to co-deliver a chemotherapy drug along with the miR-145. We investigated the potential of these nanoparticles to deliver microRNAs and our results suggest it to be a promising delivery system to restore miR-145 in pancreatic cancer cells.

Our studies demonstrating functional effects on proliferation, invasion and migration, as observed in our previous studies [4], are as a consequence of miR-145 restoration, suggesting the efficient delivery of miR-145 due to miR-145-MNPF. The biological functions of a microRNA are dependent on its interaction with its intracellular target which in the case of miR-145 is MUC13 in pancreatic cancer. We observed an effective and active routing of miR-145 into the cell through miR-145-MNPF that was sufficient to successfully deliver it to its intracellular target in an active form as was depicted by decreased MUC13 expression in cells. (Fig. 7). This was accompanied by demonstrating functional inhibitory effects on growth, invasion and motility of cancer cells (Fig. 4, 5 and 6) via inhibiting MUC13 associated oncogenic protein, HER2, $pAKT^{Ser473}$ and restoring p53 levels (Fig. 7). Our previous studies demonstrating sustained release of therapeutics from these magnetic nanoparticles [9, 10, 8] confirm that miR-145-MNPF will lead to significant and sustained release of miR-145, generating a prolonged effect on its target protein, MUC13 and functional effects on proliferation and invasion. Therefore, this magnetic nanoparticle formulation proves to be an efficient delivery technique for therapeutic intervention.

Conclusion

Our miR-145 loaded MNP formulation (miR-145-MNPF) efficiently delivers miR-145 and restores its expression in pancreatic cancer cells. Restitution of miR-145 using miR-MNPF formulation successfully inhibits its target oncogene, MUC13, thereby, suppressing tumorigenic and metastatic phenotypes of pancreatic cancer cells. Therefore, this unique magnetic nanoparticles based formulation can be efficiently used for microRNA replacement and pancreatic cancer therapy alone or in combination with conventional chemotherapy drugs. Our future goal is to further enhance the specificity of MNPs towards pancreatic cancer cells/tissues via active targeting. This will be achieved by conjugating MUC13 monoclonal antibody to the formulation which will route the formulation specifically to cancer cells having high MUC13 expression. The results from this study offer a new therapeutic strategy for pancreatic cancer treatment that warrants further investigation in future preclinical and clinical studies.

Acknowledgments

Financial support:

Subhash C. Chauhan: This work was partially supported by grants from the National Institutes of Health (R01 CA142736, U01 CA162106A, and K22CA174841); Department of Defense (PC130870) and financial support from the Kosten Foundation for pancreatic cancer research (UT 14-0558).

This work was partially supported by grants from the National Institutes of Health (R01 CA142736 to SCC, U01 CA162106A to SCC and MJ; K22CA174841 to MMY), Department of Defense (PC130870 to SCC and MJ), the College of Pharmacy 2015 Dean's Seed/Instrument Grants of the University of Tennessee Health Science Center (to SCC, MJ and MMY). Authors acknowledge the Herb Kosten Foundation for pancreatic cancer research support. The authors are also thankful to Cathy Christopherson for editorial assistance.

References

1. Siegel RL, Miller KD, Jemal A. Cancer statistics, 2016. CA: A Cancer Journal for Clinicians. 2016; 66(1):7–30. DOI: 10.3322/caac.21332 [PubMed: 26742998]
2. Wu Y, Crawford M, Mao Y, Lee RJ, Davis IC, Elton TS, et al. Therapeutic Delivery of MicroRNA-29b by Cationic Lipoplexes for Lung Cancer. Mol Ther Nucleic Acids. 2013; 2:e84.doi: 10.1038/mtna.2013.14 [PubMed: 23591808]
3. Chen C-Z. MicroRNAs as Oncogenes and Tumor Suppressors. New England Journal of Medicine. 2005; 353(17):1768–71. DOI: 10.1056/NEJMp058190 [PubMed: 16251533]
4. Khan S, Ebeling MC, Zaman MS, Sikander M, Yallapu MM, Chauhan N, et al. MicroRNA-145 targets MUC13 and suppresses growth and invasion of pancreatic cancer. Oncotarget. 2014; 5(17): 7599–609. [PubMed: 25277192]
5. Sureban SM, May R, Qu D, Weygant N, Chandrakesan P, Ali N, et al. DCLK1 Regulates Pluripotency and Angiogenic Factors via microRNA-Dependent Mechanisms in Pancreatic Cancer. PLoS ONE. 2013; 8(9):e73940.doi: 10.1371/journal.pone.0073940 [PubMed: 24040120]
6. Kent OA, Chivukula RR, Mullendore M, Wentzel EA, Feldmann G, Lee KH, et al. Repression of the miR-143/145 cluster by oncogenic Ras initiates a tumor-promoting feed-forward pathway. Genes & Development. 2010; 24(24):2754–9. DOI: 10.1101/gad.1950610 [PubMed: 21159816]
7. Gao S, Wang P, Hua Y, Xi H, Meng Z, Liu T, et al. ROR functions as a ceRNA to regulate Nanog expression by sponging miR-145 and predicts poor prognosis in pancreatic cancer. Oncotarget. 2016; 7(2):1608–18. [PubMed: 26636540]
8. Yallapu MM, Othman SF, Curtis ET, Gupta BK, Jaggi M, Chauhan SC. Multi-functional magnetic nanoparticles for magnetic resonance imaging and cancer therapy. Biomaterials. 2011; 32(7):1890–905. [PubMed: 21167595]

9. Yallapu MM, Ebeling MC, Khan S, Sundram V, Chauhan N, Gupta BK, et al. Novel curcumin-loaded magnetic nanoparticles for pancreatic cancer treatment. Molecular cancer therapeutics. 2013; 12(8):1471–80. DOI: 10.1158/1535-7163.mct-12-1227 [PubMed: 23704793]
10. Yallapu MM, Othman SF, Curtis ET, Bauer NA, Chauhan N, Kumar D, et al. Curcumin-loaded magnetic nanoparticles for breast cancer therapeutics and imaging applications. International journal of nanomedicine. 2012; 7:1761–79. DOI: 10.2147/ijn.s29290 [PubMed: 22619526]
11. Ibrahim AF, Weirauch U, Thomas M, Grünweller A, Hartmann RK, Aigner A. MiRNA replacement therapy through PEI-mediated in vivo delivery of miR-145 or miR-33a in colon carcinoma. Cancer Research. 2011; doi: 10.1158/0008-5472.can-10-4645
12. Patnaik S, Gupta KC. Novel polyethylenimine-derived nanoparticles for in vivo gene delivery. Expert Opinion on Drug Delivery. 2013; 10(2):215–28. DOI: 10.1517/17425247.2013.744964 [PubMed: 23252504]
13. Liang GF, Zhu YL, Sun B, Hu FH, Tian T, Li SC, et al. PLGA-based gene delivering nanoparticle enhance suppression effect of miRNA in HePG2 cells. Nanoscale research letters. 2011; 6:447.doi: 10.1186/1556-276x-6-447 [PubMed: 21749688]
14. Khan S, Ebeling MC, Chauhan N, Thompson PA, Gara RK, Ganju A, et al. Ormeloxifene suppresses desmoplasia and enhances sensitivity of gemcitabine in pancreatic cancer. Cancer Res. 2015; 75(11):2292–304. DOI: 10.1158/0008-5472.CAN-14-2397 [PubMed: 25840985]
15. Khan S, Chauhan N, Yallapu MM, Ebeling MC, Balakrishna S, Ellis RT, et al. Nanoparticle formulation of ormeloxifene for pancreatic cancer. Biomaterials. 2015; 53:731–43. DOI: 10.1016/j.biomaterials.2015.02.082 [PubMed: 25890768]
16. Chauhan SC, Vannatta K, Ebeling MC, Vinayek N, Watanabe A, Pandey KK, et al. Expression and functions of transmembrane mucin MUC13 in ovarian cancer. Cancer Res. 2009; 69(3):765–74. DOI: 10.1158/0008-5472.CAN-08-0587 [PubMed: 19176398]
17. Jaggi M, Rao PS, Smith DJ, Wheelock MJ, Johnson KR, Hemstreet GP, et al. E-cadherin phosphorylation by protein kinase D1/protein kinase C{mu} is associated with altered cellular aggregation and motility in prostate cancer. Cancer Res. 2005; 65(2):483–92. [PubMed: 15695390]
18. Liang W, Gong H, Yin D, Lu S, Fu Q. High-Molecular-Weight Polyethyleneimine Conjuncted Pluronic for Gene Transfer Agents. Chemical and Pharmaceutical Bulletin. 2011; 59(9):1094–101. DOI: 10.1248/cpb.59.1094 [PubMed: 21881251]

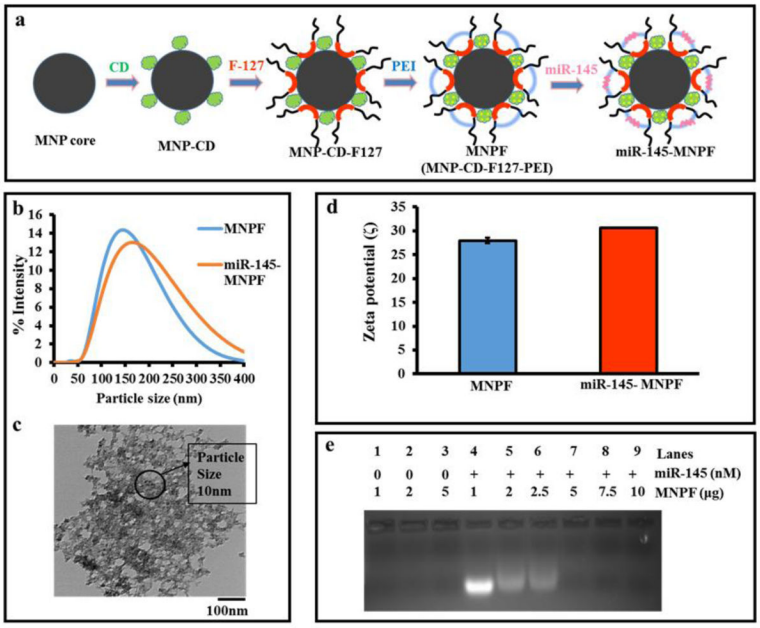

Fig. 1. Generation of miR-145-MNPF and its physicochemical characterization

a) Schematic representation of the generation of miR-145-MNPF. Co-precipitation of iron oxide nanoparticles followed by β-cyclodextrin and F127 polymer coatings leads to MNP nanoformulation (MNPF). Surface modification of MNPF was done with Polyethylenimine (PEI) and conjugated with miR-145 by incubation in 1mg/ml MNPF in 0.9% NaCl solution. b) Average miR-145-MNPF aggregative size is 163 nm) Transmission electron microscopic (TEM) image of miR-145-MNPF showing individual particle size of 8–10 nm. d) Zeta potential of miR-145-MNPF 30.63 mV. **e)** Gel retardation assay by agarose gel electrophoresis showing the formation of a complex between MNPF and miR-145 through electrostatic interaction. Complex formation is seen in the lane 5 and the complexation further increases in the lanes 6–9 with the increase in the concentration of MNP (2–10 μg).

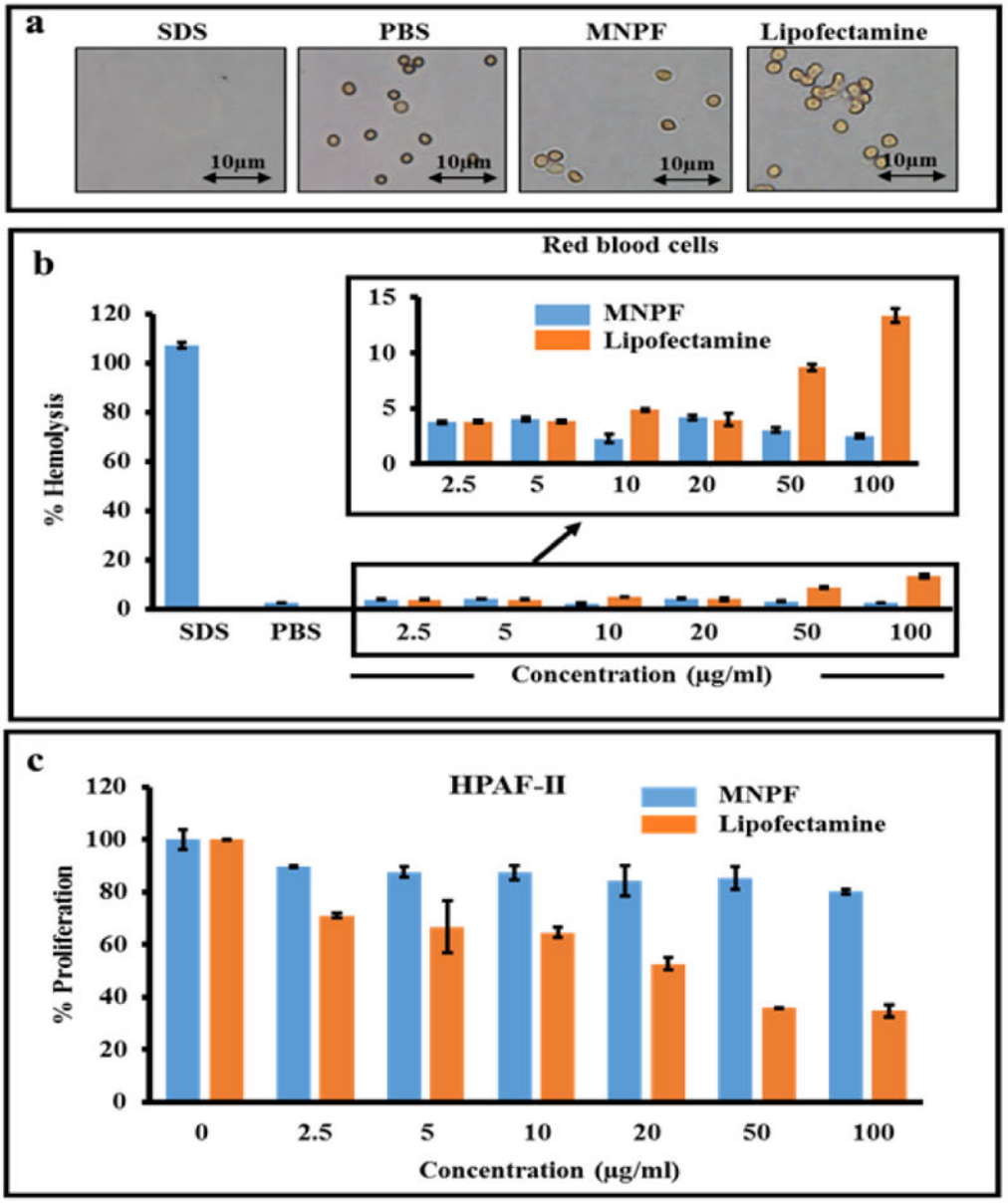

Fig. 2. Evaluation of hemocompatibility and toxicity using RBCs and HPAF-II cells

Hemolysis was performed by incubating MNPF in red blood cells for two hours. **a)** Images showing the effect of MNPF and lipofectamine on RBCs. **b)** Cells were centrifuged and supernatant collected for analysis. PBS and SDS were taken as negative and positive controls, respectively. **c)** Toxicity of MNPF and lipofectamine was compared in pancreatic cancer cells, HPAF-II using cell proliferation assay.

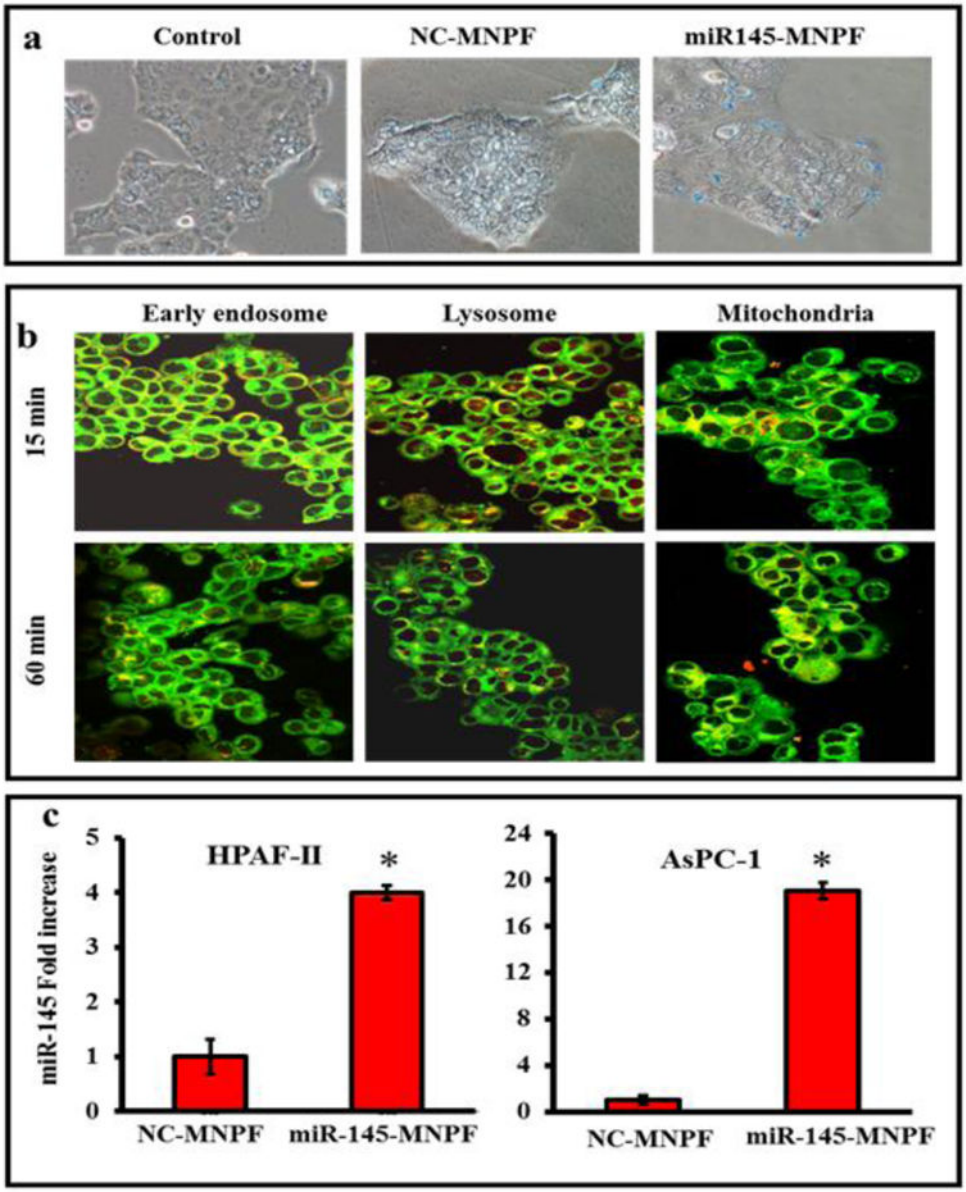

Fig. 3. Restitution of miR-145 in pancreatic cancer cells using miR-145-MNPF

a) Cellular uptake of miR-145-MNPF was determined by Prussian blue staining. Pancreatic cancer cells were seeded and treated with MNPF, NC-MNPF, miR-145-MNPF. After 24 hours, cells were stained with Prussian blue reagent and photographed under phase contrast microscopy (Original Magnifications 100X. **b)** Determination of fate and subcellular localization of Coumarin-6 dye (green color) labelled MNPF nanoformulation (Original Magnifications 400X). HPAF-II pancreatic cancer cells (1×10^5/well) were exposed to Coumarin-6 labelled MNPF for 1 h. Cells were stained with Transferrin from Human Serum, Texas Red® Conjugate, LysoTracker Red and Mito Tracker Red, as markers for endosome, lysosome, and mitochondria, respectively. Green color indicated uptake of Coumarin-6 labelled MNPF and yellow color indicated co-localization of Coumarin-6

labelled MNPF in endosome, lysosome and mitochondria. **c)** miR-145 restoration in cells was confirmed using Taqman probes by q-PCR. Expression level of miR-145 was observed in cells after 48 hours of transfection. Results represented as fold increase of miR-145 in comparison with NC-MNPF. Bars represent mean ± SEM, **n=3**, *$P<0.05$.

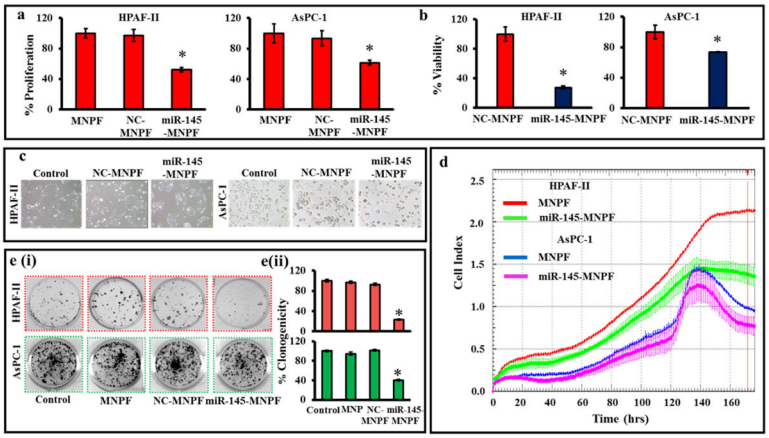

Fig. 4. miR-145 restoration using miR-145-MNPF inhibits proliferation and colonogenicity in pancreatic cancer cells

a) Effect of miR-145-MNPF on cell growth and proliferation was performed using cell counting Kit-8 in HPAF-II and AsPC-1 cells. **b)** Effect of miR-145-MNPF on cell viability by counting the cells using Cell Countess in HPAF-II and AsPC-1 cells. **c)** Representative images of cells morphology after treated with miR-145-MNPF for 48 h using phase contrast microscopy. **d)** Effect of miR-145-MNPF treatment on cell proliferation with respect to time (h) was also confirmed by xCELLigence RTCA. **e)** HPAF-II and AsPC-1 cells were treated with miR-145-MNPF and incubated for 12 days for investigating the colony forming ability of the cells. Colonies were counted and plotted as percent colonogenicity. Percent inhibition of clonogenicity of miR-145-MNPF transfected cells as compared with NC-MNPF. Bars represent mean ± SEM, **n=3**,**P*<0.05.

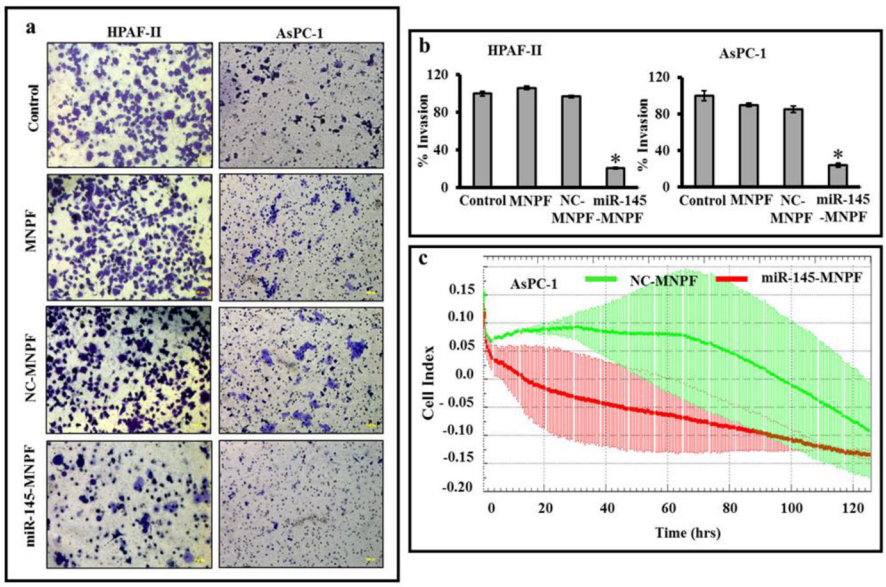

Fig. 5. Effect of miR-145-MNPF on cellular invasion in pancreatic cancer cells

a) Matrigel Invasion Assay. Cells treated with MNPF, NC-MNPF and miR-145-MNPF were plated into the top chamber of the well in serum free media with a Matrigel-coated membrane. 10% FBS was added to the lower chamber as a chemoattractant. After 48 hours of incubation, invaded cells were identified by crystal violet staining followed by imaging. **b)** Data represented as percent inhibition of invasion of miR-145-MNPF transfected cells as compared with MNPF. **c)** Effect of miR-145-MNPF on cellular invasion ability was confirmed using xCELLigence system. Bars represent mean ± SEM, **n=3**, **P*<0.05.

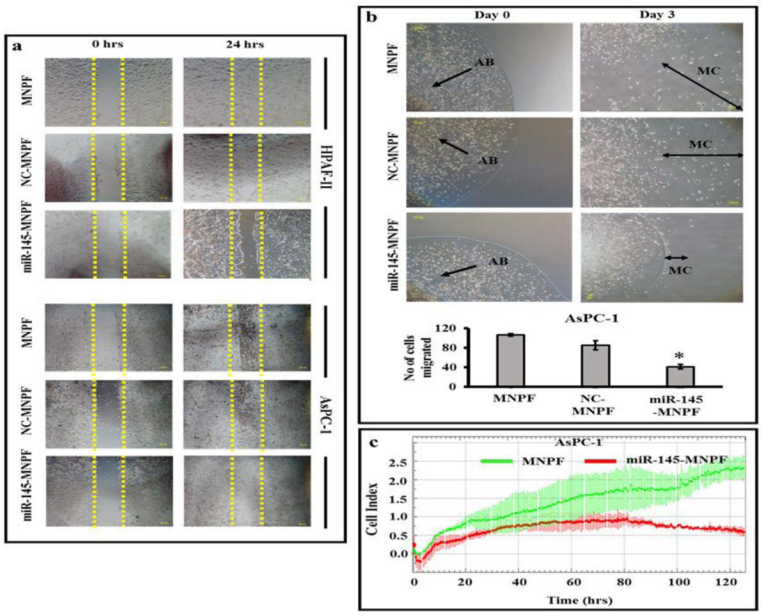

Fig 6. Effect of miR-145-MNPF on cell migration ability of pancreatic cancer cells

a) Cell scratch assay. HPAF-II and AsPC-1 cells treated with MNP-NC and miR-145-MNPF were seeded overnight followed by scratch. The scratch was monitored for closure following MNP-NC or miR-145-MNP treatment which was followed by photographing at 24 h. **b)** Agarose Bead Assay. HPAF-II and AsPC-1 cells were mixed into agarose solution and 20 μl dropped onto fibronectin/bovine serum albumin coated plates. Number of migratory cells (MC) from agarose beads (AB) were photographed (day 0 and day 3) and quantified by counting the MC cells compared to control. **c)** Effect of miR-145-MNPF on cell migration ability was confirmed using xCELLigence system. Bars represent mean ± SEM, **n=3**, **P*<0.05.

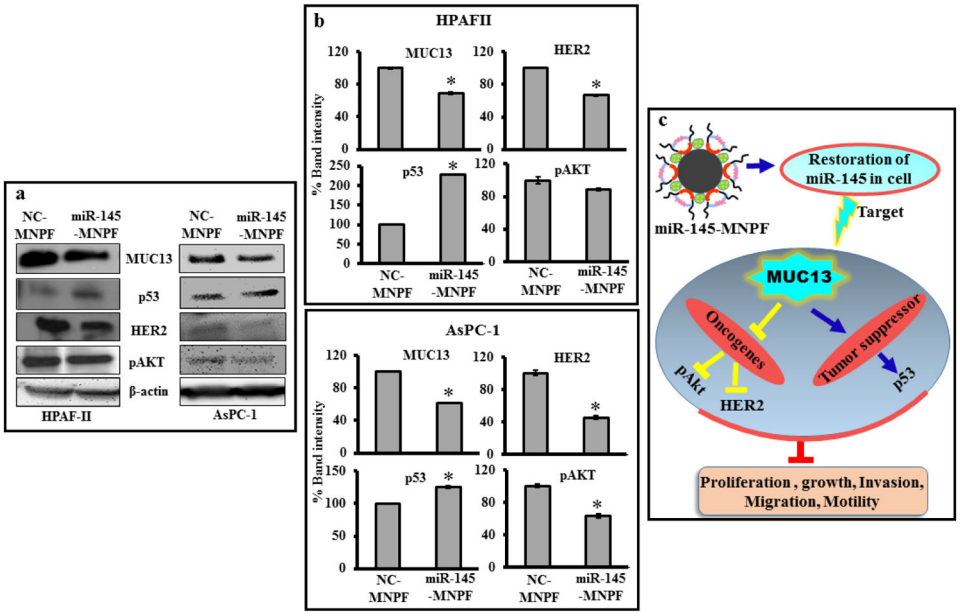

Fig. 7. Effect of miR-145-MNPF on MUC13 and its associated targets

a) HPAF-II and AsPC-1 was treated with NC-MNPF or miR-145-MNPF. Whole cell lysate were immunoblotted for MUC13, HER2, pAKT^{Ser473} and p53 proteins. β-actin was used as a loading control. **b) Bars represent the** densitometric analysis of the blots by GelQuant. Bars represent mean ± SEM, n=3, *P<0.05. c) Schematic representation illustrating the effects of miR-145 restitution using miR-145-MNPF.